

Solid-state effects on Ag in dilute alloys revealed by Cooper-minimum photoemission

R. J. Cole, J. A. Evans, L. Duò, A. D. Laine, P. S. Fowles, and P. Weightman

*Department of Physics, University of Liverpool, Liverpool L69 3BX, United Kingdom
and Surface Science Research Centre, University of Liverpool, Liverpool L69 3BX, United Kingdom*

G. Mondio

*Istituto di Struttura della Materia della Facoltà di Scienza, Università di Messina, Cassella Postale 56,
I-98166 Villa San Agata, Messina, Italy*

D. Norman

*Science and Engineering Research Council, Daresbury Laboratory, Warrington WA4 4AD, United Kingdom
(Received 28 August 1991; revised manuscript received 6 January 1992)*

Synchrotron-radiation photoemission has been used to study the region of the Cooper minimum of the Ag $4d$ states in the random substitutional alloys $\text{Al}_{95}\text{Ag}_5$ and $\text{Cd}_{97}\text{Ag}_3$. We have developed an internally consistent analysis by relating the intensity of the Ag $4d$ states to the intensity of the step at the Fermi level. The results are compared with previously published theoretical calculations for atomic Ag and experimental data for atomic Ag and solid Ag, and for a submonolayer thickness of Ag deposited on a Si(111) substrate. The Ag $4d$ Cooper minimum is perturbed from its atomic values owing to hybridization of the Ag $4d$ wave function with that of the neighbor atoms. We use this to deduce details of how silver is bonded in these different systems. It is shown that the Ag in dilute Al-Ag is quite similar to atomic Ag while in Cd-Ag the Ag atoms are somewhat more perturbed than in metallic Ag. In the Cd-Ag alloy, the $4d$ cross section per atom for Ag is lower than for Cd throughout the photon-energy range of 40–170 eV.

I. INTRODUCTION

Although there are several experimental techniques that provide information on the densities of states (DOS) in metals and their alloys, there are few that can provide information on the associated wave functions. One way of probing the character of valence wave functions is to measure the photoionization cross section σ as a function of photon energy $h\nu$. For wave functions which contain a radial node σ can show significant changes as the photon energy is varied and cancellation in matrix element integrals for transitions to particular final states causes a pronounced minimum in σ , the Cooper minimum (CM).^{1,2} These occur for any initial-state orbital where the principal quantum number n and the angular momentum l are related by $n > l + 1$, such as $3p, 4p, 4d$. Since the CM effect is very sensitive to the details of the initial-state wave function, $\sigma(h\nu)$ in the CM region is a valuable probe of the way in which valence wave functions are modified by solid-state effects and by the chemical environment.

The advent of synchrotron radiation as a tunable excitation source has made it possible to exploit the CM effect, both to separate different orbital contributions to the local DOS for a wide variety of alloys^{3–7} and metal-semiconductor interfaces^{8–10} involving $4d$ and $5d$ elements, and to correlate changes in the form of $\sigma(h\nu)$ for an orbital of a given atom in different environments to changes in electronic structure.^{11–19}

In this work we have studied the CM of Ag $4d$ states in a dilute alloy with an sp metal (Al) and with another, d -

band metal (Cd), in both of which the Ag impurity forms a virtual bound state.^{20,21} The proportion of Ag in the alloys was 5 at. % in Al and 3 at. % in Cd, sufficiently dilute that the Ag atoms are well separated and noninteracting. The CM results are compared with previously published theoretical and experimental cross-section data on other systems involving Ag, and we relate the changes in the Ag $4d$ CM in these alloys to the local electronic structure.

In the next section, we describe our experimental methods, while Sec. III contains the results and analysis. The findings are discussed and compared with theoretical calculations and the results of experiments on other systems in Sec. IV.

II. EXPERIMENTAL PROCEDURE

The experiments were performed on beamline 6.1 at the Daresbury Synchrotron-Radiation Source. The pressure in the experimental chamber was in the low 10^{-10} mbar region throughout the course of the experiments, and the samples were kept at room temperature. Photoelectron spectra were collected using a commercial (Perkin-Elmer) double pass cylindrical mirror analyzer (CMA) operated in fixed transmission mode. Specimens of the random substitutional alloys $\text{Al}_{95}\text{Ag}_5$ and $\text{Cd}_{97}\text{Ag}_3$ were prepared by melting together high-purity components in an atmosphere of argon. No loss of weight occurred during their fabrication. The same specimens have been studied previously^{22,23} using x-ray excited photoemission and Auger electron spectroscopies. The speci-

mens were cleaned by mechanical scraping with a tungsten carbide blade. Photoemission from the O 2s level was monitored as a measure of surface cleanliness and a new surface was created when an increase was seen in that region. Using photon energies near to the O 2s threshold, this method is more sensitive than conventional Auger electron spectroscopy excited by higher-energy electrons. The upper level of contamination is less than 0.1 monolayers. For the CM experiments we used photons in the energy range 40–170 eV, selected by a plane grating monochromator²⁴ and incident on the samples at an angle of $\sim 60^\circ$ from the normal. The variation of the photon flux incident on the sample as a function of photon energy and due to the decay with time of the storage beam current is corrected by dividing each spectral point by the current measured at a tungsten grid situated between the monochromator and the sample. There are three components to the experimental resolution ΔE : the natural width of a feature, the bandwidth of the electron energy analyzer, and the bandwidth of the photon monochromator. ΔE was measured by fitting the Fermi edge of each spectrum to a Fermi-Dirac distribution convolved with a Gaussian of width ΔE . The resolution was found to increase with photon energy from 0.5 eV at $h\nu=40$ eV to 1.8 eV at $h\nu=170$ eV.

III. RESULTS AND ANALYSIS

The experimental spectra, normalized to the intensity of the step at the Fermi level, are shown in Fig. 1. The Ag 4d peaks lie 6.4 eV below the Fermi level ϵ_F and their intensity variation with photon energy is clearly visible in the raw data. The peaks at 12-eV binding energy in the $h\nu=110$ eV spectrum and at 13-eV binding energy in the 60-eV spectrum for the Al₉₅Ag₅ alloy [see Fig. 1(a)] arise from the photoemission of Al 2s and Al 2p states, respectively, excited by second-order photons. As can be seen from the spectrum excited by 60-eV photons in Fig. 1(b), the Cd 4d band is at a binding energy of 11 eV.

The measured photoelectron intensity $I(h\nu)$ of a state has been related to its cross section $\sigma(h\nu)$ by Rossi *et al.*¹⁰ by the expression

$$I(h\nu) \propto \sigma(h\nu)\lambda(E_{\text{kin}})\xi(E_{\text{kin}})\Phi(h\nu)F(\chi, \eta, \kappa, \lambda), \quad (1)$$

where $\lambda(E_{\text{kin}})$ is the photoelectron escape depth, and $\xi(E_{\text{kin}})$ is the efficiency of the photoelectron detector as functions of photoelectron kinetic energy E_{kin} . The factor F is a function of the angle of incidence of the beam χ and allows for reflection at the sample surface and refraction of the beam within the escape depth; hence F is also a function of λ and of the complex index of refraction of the sample $(\eta + i\kappa)$.

There are formidable difficulties in obtaining accurate correction functions to relate $I(h\nu)$ to $\sigma(h\nu)$. The relationship between data collected with a CMA and the total cross section has been explored by del Pennino *et al.*²⁵ This work shows that, in our photon-energy range, it is possible to calculate F at the average acceptance angle of the spectrometer, and thus that the effective σ as measured in our experiment can be directly compared with

the true differential cross section. Our experimental geometry, with photons incident at an angle of 60° , is close to the limit in which $F \rightarrow 1$. However, to avoid the difficulties in obtaining *absolute* values for σ , we have used the intensity of the free-electron-like step lying just below the Fermi energy I_{ϵ_F} as an internal reference in

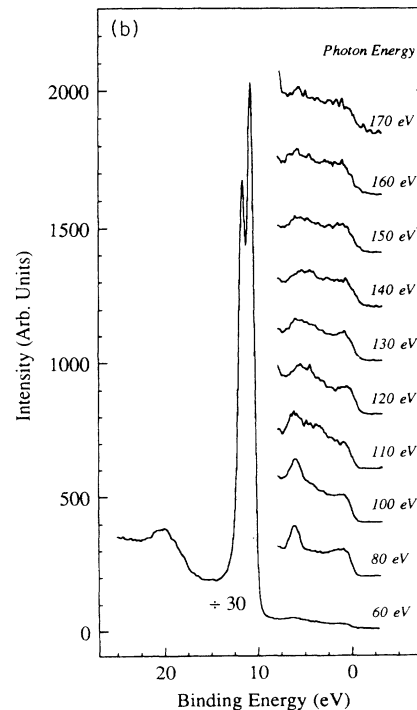
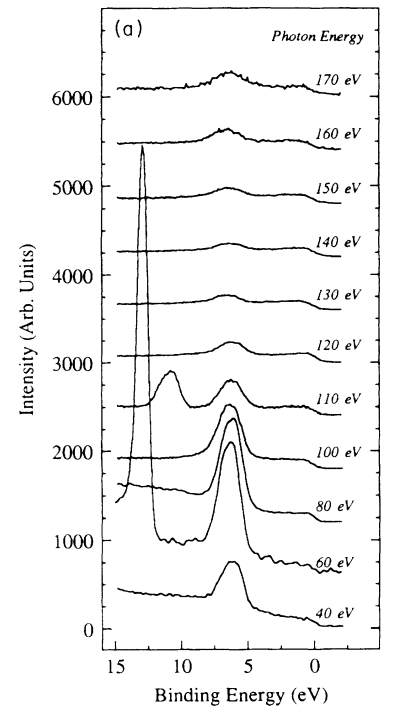


FIG. 1. Valence-band photoelectron spectra, normalized to the intensity of the Fermi level, for (a) Al₉₅Ag₅ and (b) Cd₉₇Ag₃ at different photon energies.

each spectrum. Since the Ag $4d$ states in each alloy are bound by only 6.4 eV, the transmission function of the analyzer and the electron escape depths will be, to a good approximation, equal for the kinetic energies of the Ag $4d$ and the host Fermi energy photoelectrons in each spectrum. Thus, by measuring the ratio of intensities I_{4d}/I_{ϵ_F} we are directly measuring the ratio of cross sections $\sigma_{4d}/\sigma_{\epsilon_F}$, since all the correction terms in (1) cancel. σ_{4d} is then easily obtained,

$$\sigma_{4d} = \sigma_{\epsilon_F} \frac{I_{4d}}{I_{\epsilon_F}}. \quad (2)$$

From electronic structure calculations²⁶ for pure Al metal, we expect the states at the Fermi level in $\text{Al}_{95}\text{Ag}_5$ to have predominantly Al $3p$ character. Similarly, we expect Cd $5s$ character at the Fermi level in $\text{Cd}_{97}\text{Ag}_3$. Assuming that their cross sections are well represented by Al $3p$ and Cd $5s$ atomic values, respectively, we can deduce $\sigma_{4d}(h\nu)$ using theoretical calculations²⁷ for Al $\sigma_{3p}(h\nu)$ and Cd $\sigma_{5s}(h\nu)$. It can be seen that this assumption holds well for Si, the nearest neighbor to Al in the Periodic Table, by comparing Fig. 9 of Ref. 10 with the calculated cross section²⁷ for atomic Si $3p$ levels in the energy range 70–200 eV. This method of analysis works well in this study because the variation of the Al $3p$ and Cd $5s$ cross sections is much less than that of the $4d$ orbitals of Cd and Ag.

The Ag $4d$ levels are degenerate in energy with part of the host valence band, so to deduce the intensity of the Ag $4d$ states a way is needed of separating these contributions. We have modeled the impurity electronic structure using simple Hamiltonians, namely those of Anderson²¹ (for $\text{Al}_{95}\text{Ag}_5$) and of Clogston and Wolff^{28,29} (for $\text{Cd}_{97}\text{Ag}_3$), which represent the impurity-host interactions with a small number of parameters. While these models have physical simplicity and have been successfully applied to many alloys, their value and validity is of secondary importance here since we are only concerned with the intensity of the impurity $4d$ states rather than the detailed alloy band structure. The model DOS is used only to determine the Ag $4d$ intensity in a consistent manner.

The Anderson model²¹ was introduced to explain the existence of localized magnetic moments in dilute alloys and has been successful in describing d -electron metal impurities in free-electron metal hosts. It allows the mixing of the impurity d states with the host sp band and, for a magnetic impurity, includes the Coulomb exchange interaction between two d electrons of opposite spin on the same site. The impurity line shape has a width determined by the extent of the d - sp hybridization. In $\text{Al}_{95}\text{Ag}_5$ the Ag $4d$ -derived virtual bound state (VBS) has a binding energy of 6.4 eV and width 0.5 eV [see Fig. 2(a)]. We fitted the Anderson model VBS and the Al valence band, to each photoelectron spectrum to determine the ratio of their intensities, and hence of their cross sections.

The Clogston-Wolff model^{28,29} uses a tight-binding Hamiltonian appropriate for a d -metal impurity in another d -metal host. The host-host $4d$ hopping is assumed to

be equal to the host-impurity $4d$ hopping but there is a shift Δ of the d -electron energy for an impurity site. The impurity DOS consists of a sharp peak shifted from the host d band by an amount Δ and a small contribution under the host d band. For the Ag impurity in $\text{Cd}_{97}\text{Ag}_3$, $\Delta=4.7$ eV, and there is a broadening of 0.15 eV due to Anderson d - sp hybridization [see Fig. 2(b)]. These parameters correspond to approximately 3% of the Ag $4d$ intensity lying under the Cd $4d$ band. This prediction cannot be tested by photoemission, but the Ag

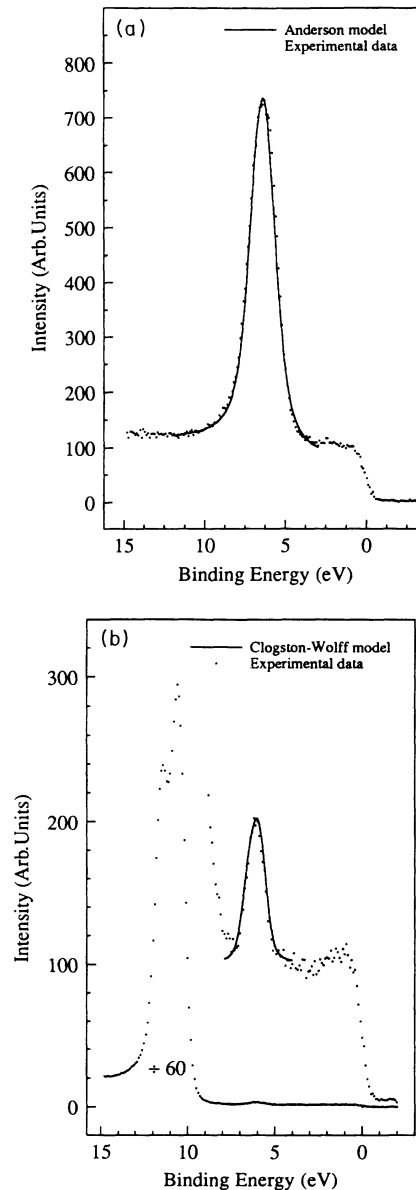


FIG. 2. (a) Experimental valence-band photoelectron spectrum, taken at $h\nu=100$ eV, for $\text{Al}_{95}\text{Ag}_5$, compared to the results of a calculation for the Ag virtual bound state using the Anderson model (Ref. 21). (b) Experimental valence-band photoelectron spectrum, taken at $h\nu=80$ eV, for $\text{Cd}_{97}\text{Ag}_3$, compared to the results of a calculation for the Ag virtual bound state using the Clogston-Wolff model Hamiltonian (Refs. 28 and 29).

$M_{4,5}N_{4,5}N_{4,5}$ Auger spectral profile is very sensitive to the Ag $4d$ intensity in the region of the host d band [since $\Delta \sim U(LSJ)$, where $U(LSJ)$ are the correlation energies of the two-hole final state LSJ multiplets], and Auger spectroscopy has been used to show that the Clogston-Wolff model predicts the mixing into the host d band quite accurately for this²³ and other alloys.³⁰

In Figs. 3–5 are plotted the photoionization cross sections σ_{4d} for a variety of systems. The curves have been normalized to 100 at their maxima and plotted on a logarithmic scale to emphasize the different depths of $4d$ CM. Figure 3 displays previously published data for solid metallic¹⁷ Ag and gas phase atomic¹⁶ Ag, compared with atomic Hartree-Fock-Slater (HFS) calculations.²⁷ Figure 4 shows the Ag $4d$ states in different solid environments with our data for Ag in $Cd_{97}Ag_3$ and Ag in $Al_{95}Ag_5$ compared with that for metallic¹⁷ Ag and for a submonolayer coverage of Ag on Si(111) (Ref. 13). For the $Cd_{97}Ag_3$ alloy, we measured the $4d$ cross sections of both the impurity and the host: in Fig. 5 are contrasted our data for the host Cd states in this alloy with metallic Ag (Ref. 17), and Ag on Si(111) (Ref. 13). The maximum for Cd in Cd-Ag may not be quite correctly depicted since it occurs at about 90 eV, and data were not collected for Cd-Ag at this photon energy.

Whereas Figs. 3–5 are used to display the different depths of $4d$ CM for different atoms and environments, Fig. 6 shows the direct comparison between Cd and Ag $4d$ cross-section absolute magnitudes in the $Cd_{97}Ag_3$ alloy. As for Figs. 3–5, σ modulation due to variations in the Fermi energy states is removed using (2) but the curves are not independently normalized to 100 at their maxima. Using the known concentrations of the Cd-Ag alloy, the Cd and Ag $4d$ cross sections *per atom* can be determined. Although the units are arbitrary, no relative

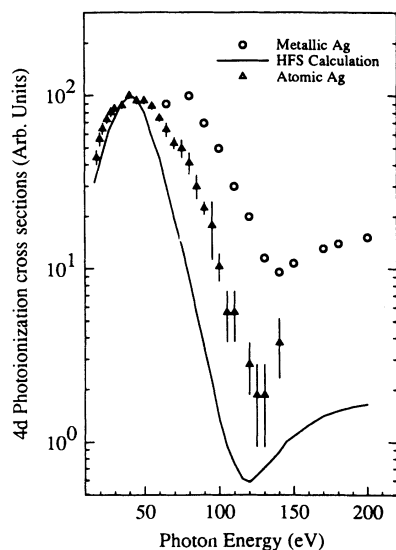


FIG. 3. The photon-energy dependence of the cross section of Ag $4d$ states for metallic Ag (Ref. 17), atomic Ag (Ref. 16), and Hartree-Fock-Slater calculations (Ref. 27) for free atomic Ag, normalized to a maximum of 100 for each set of data.

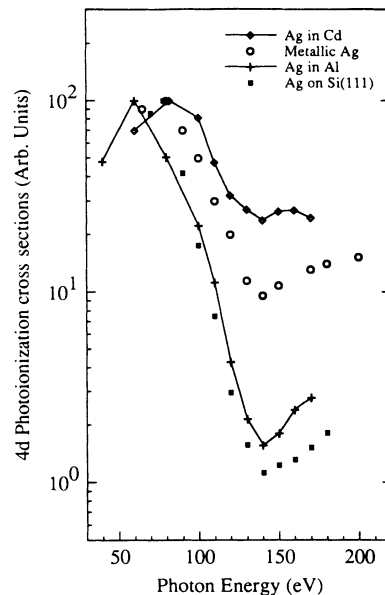


FIG. 4. The photon-energy dependence of the photoionization cross section of Ag $4d$ states from our experiments on $Al_{95}Ag_5$ and $Cd_{97}Ag_3$, together with the experimental data for metallic Ag (Ref. 17) and Ag on Si(111) (Ref. 13). All data have been set to a maximum of 100.

scaling of the two curves in Fig. 6 has taken place, and since the Ag and Cd states were measured in the same spectrum for each photon energy, the cross sections *per atom* for the Cd and Ag $4d$ states can be plotted on strictly the same scale. We are then able to deduce information about the environmental effects on the absolute mag-

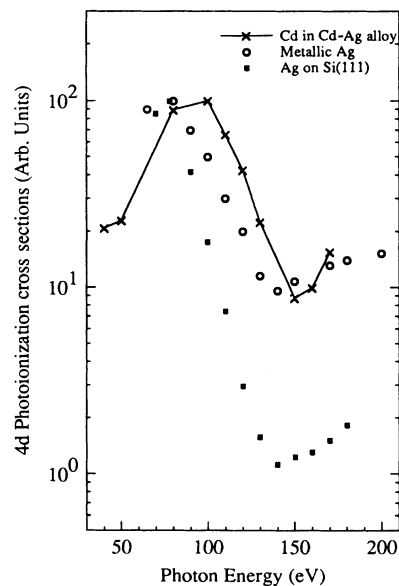


FIG. 5. The photon-energy dependence of the photoionization cross section of Cd $4d$ states from our experiments on $Cd_{97}Ag_3$, together with experimental data for the $4d$ states of metallic Ag (Ref. 17) and Ag on Si(111) (Ref. 13). All data have been set to a maximum of 100.

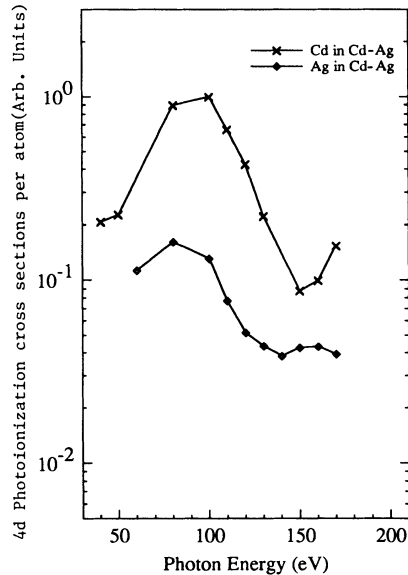


FIG. 6. The photon-energy dependence of the photoionization cross section *per atom* of Cd and Ag 4*d* states from our experiments on Cd₉₇Ag₃.

nitudes of 4*d* cross sections, as well as on the depths of the CM.

The 4*d* orbitals in the different environments presented here all exhibit CM in the 120–150-eV photon-energy range, but with widely varying depths from maximum to minimum. In the next section we discuss what this means in terms of the nature of the 4*d* wave functions. Table I gives the values of the range *r* of the cross section [$r = \log_{10}(\sigma_{\max}/\sigma_{\min})$] for 4*d* orbitals in various bonding environments.

IV. DISCUSSION

In this section we start by focusing on the differences between the shape of the Cooper minima for different systems, and particularly concentrate on the energy position of the minimum and the range *r*. The variation of

TABLE I. The range [$r = \log_{10}(\sigma_{\max}/\sigma_{\min})$] of the 4*d* Cooper minimum in various systems.

	<i>r</i>	Reference
Ag atoms (theory)	2.3	27
Ag atoms	1.7	16
Ag on Si	1.9	10,13
Ag in Al-Ag	1.8	This work
Ag metal	1.0	17
Ag metal	1.1	10,13
Ag metal	1.5	11
Ag metal	1.7	12
Ag metal	1.7	18
Ag in Cd-Ag	0.5	This work
Cd in Cd-Ag	1.1	This work

$\sigma_{4d}(h\nu)$ with atomic number *Z* is very weak for the 4*d* orbitals of atoms.²⁷ In atomic Ag (Refs. 16 and 27) the minimum occurs at $h\nu=135$ eV, and the depth of the CM covers two orders of magnitude ($r=2$). The Ag 4*d* orbitals at the submonolayer Ag on Si(111) interface and the Mo 4*d*_{z²} orbitals in solid MoS₂ are both believed to have predominantly atomic character.^{10,13,15,17} The $\sigma(h\nu)$ variation has been studied for both these orbitals in the CM region and has been found to be very similar to atomic cross-section calculations.^{10,13,15,17,27} There is a large experimental uncertainty associated with the only Ag gas phase cross-section data currently available,¹⁶ which gives $r \sim 1.7$ (see Fig. 3), compared with $r \sim 1.9$ for Ag on Si.^{10,13,17} Atomic HFS cross-section calculations²⁷ show a slightly deeper CM than that determined experimentally, but it is known that the depth of the CM is a very stringent test of the wave functions used in the theoretical calculations.

For 4*d* elements in the metallic phase there is significant *d-d* overlap which distorts the atomic orbitals. The CM effect, depending crucially on cancellation in matrix element integrals, is unique in its ability to detect the onset of distortion of the 4*d* wave function (ψ_{4d}) in the region of the radial minimum as *Z* decreases, and thus the bandlike character of the 4*d* states is increased. The noble metal Ag has a filled 4*d* band which is bound by about 4–6 eV, and the radial node in ψ_{4d} lies well within the region of significant *d-d* overlap. Thus Ag metal retains a clear CM (at $h\nu=140$ eV), although the solid-state effect is seen to reduce the depth of the minimum by about one order of magnitude.

Table I shows that different values have been previously published for metallic Ag. The work reported in Refs. 10 and 13, and that of Ref. 17, finds $r \sim 1.0$, while other studies^{11,12,18} report $r \sim 1.6$. We did not measure metallic Ag, but note that Refs. 11 and 12 do not specify the incident geometry and the method used to extract σ from the data. In Ref. 18, taking the quoted value of *r*, the spectra published show a surprisingly large variation in σ_{4s} that is not found in other studies. Further, we find a value of $r \sim 1.1$ for the 4*d* states of Cd in the Cd₉₇Ag₃ alloy. All these points support the view that $r \sim 1.0$ in Ag. The wide discrepancy between the values found by different groups serves to highlight the need for an alternative to calculating the correction factors for σ , such as the approach taken in this paper. We also comment that the present study is concerned with comparing Ag in a solid-state environment (such as solid metallic Ag) and Ag in an atomiclike environment [such as Ag on Si(111)]. The only data reported in the literature for both these systems measured together are those of Refs. 10, 13, and 17. There the σ values for the two different cases have been evaluated in the same way, and therefore only in those works are the data truly comparable. These experiments agree in their values of $r \sim 1.0$ for Ag metal and $r \sim 1.9$ for the Ag/Si(111) interface. Experimental data for atomic¹⁶ Ag and one of the published measurements of solid-state¹⁷ Ag are shown in Fig. 3, together with the HFS atomic cross-section calculations of Yeh and Lindau.²⁷ The 4*d* orbitals in metallic Ag have largely atomic

character, but σ_{4d} in the CM region still shows sensitivity to the d - d interaction.

On decreasing Z , the $4d$ states approach the Fermi level, become more extended, and have increased sp character. For Mo metal, σ_{4d} varies very weakly with photon energy and there is no clear CM, but only a slight shoulder shifted to higher $h\nu$ by ~ 50 eV.¹³ This dramatic modification of $\sigma_{4d}(h\nu)$ has been explained in terms of severe distortion of the behavior of ψ_{4d} near the radial node.¹³

Thus the atomic $4d$ CM effect is believed to be present in solid-state systems for orbitals which are unperturbed from their atomic form. The CM effect is also thought to be very sensitive to the extent to which the bonding environment distorts the radial wave function of an orbital. We consider the results for $\text{Al}_{95}\text{Ag}_5$ and $\text{Cd}_{97}\text{Ag}_3$ in light of these observations.

A. Al-Ag

Figure 4 shows the experimental cross-section data for the Ag $4d$ states in $\text{Al}_{95}\text{Ag}_5$, along with experimental data for metallic Ag (Ref. 17) and for submonolayer Ag on Si(111) (Ref. 13). The ordinate scale is plotted logarithmically to emphasize the differences in the CM region. Since the alloy is dilute, the Ag $4d$ orbitals do not overlap significantly. The $4d$ levels are, however, broadened by hybridization with the host sp band. The $\sigma_{4d}(h\nu)$ curve for Ag in $\text{Al}_{95}\text{Ag}_5$ shows a dramatic CM at $h\nu=140$ eV, with $r=1.8$ (see Table I), which is very similar to that of Ag at the Ag/Si(111) interface and for atomic Ag. This suggests that the Ag $4d$ wave functions in $\text{Al}_{95}\text{Ag}_5$ are not significantly perturbed from the atomic phase.

B. Cd-Ag

More significant changes are expected in alloying Ag in the $4d$ metal Cd, although it is hard to predict intuitively the extent to which the Ag $4d$ wave functions are distorted by the presence of the host d band. Cd is adjacent to Ag in the Periodic Table and, though the $4d$ states in Cd metal are 11 eV below the Fermi level, they are still substantially influenced by band structure and have a width of ~ 3.6 eV. As such, $\sigma_{4d}(h\nu)$ for Cd metal may be expected to exhibit a clear CM but with a reduced depth, in a similar manner to Ag metal. In $\text{Cd}_{97}\text{Ag}_3$ the perturbation of the host d band due to the dilute impurity will be very weak, and so the Cd $4d$ states in the alloy should have the same form of $\sigma_{4d}(h\nu)$ as pure Cd metal. $\sigma_{4d}(h\nu)$ for the Cd $4d$ states is shown in Fig. 5. The depth of the minimum is given by $r=1.1$, which is similar to the value for metallic Ag (Refs. 10, 13, and 17) of ~ 1.0 (see Table I). This suggests that although the $4d$ states of Ag impurities in Cd have a slight energy shift with respect to the Cd d band, the $4d$ radial wave function on both host and impurity lattice sites in the $\text{Cd}_{97}\text{Ag}_3$ alloy will suffer similar distortion as in a pure Ag (or indeed Cd) lattice.

Cd is the cutoff point for $4d$ bandlike character in the fifth row of the Periodic Table,³¹ and the Cd $4d$ states show a clear doublet with significant contributions from

the atomic spin-orbit coupling [see Fig. 1(b)]. In the adjacent element In, the $4d$ states have atomic spin-orbit splitting and can be considered to have evolved into the core. The Ag VBS is narrow and only a small percentage of its intensity is degenerate with the Cd $4d$ band. However, this information on the DOS does not give a clear indication of the extent to which the overlap between the Ag and Cd $4d$ wave functions causes a delocalization of the Ag $4d$ wave function. If this overlap is small, we expect the Ag $4d$ wave functions to be highly localized and perhaps atomlike as in $\text{Al}_{95}\text{Ag}_5$. If the overlap is substantial, the Ag $4d$ states could be quite extended. The CM experiments provide a useful insight into this issue, since the CM is very sensitive to the distortion of the radial wave function and so directly probes the effect of the Cd d band on the Ag $4d$ wave function. Our data show that the Ag VBS exhibits a CM at $h\nu=140$ eV (Fig. 4), but with greatly reduced depth, $r=0.5$. The range of the CM is more than an order of magnitude smaller than for the Al-Ag alloy and is more reminiscent of Mo metal. This suggests that the Ag $4d$ states in $\text{Cd}_{97}\text{Ag}_3$ are heavily involved in d - d bonding, and ψ_{4d} is consequently severely perturbed in the region of the radial node.

Study of the $\text{Cd}_{97}\text{Ag}_3$ alloy provides an opportunity of measuring $\sigma(h\nu)$ of the same subshell in two different environments on strictly the same scale, which is completely independent of any correction procedure used. The variation of σ_{4d} with $h\nu$ for Ag and Cd sites is shown in Fig. 6 without normalization. Our data reveal that σ_{4d} for an Ag site is greatly reduced with respect to its value for the Cd sites throughout the photon-energy range. This implies that the standard analysis of cross-section data by normalizing $\sigma(h\nu)$ curves at their maxima and explaining their differences solely in terms of the modification of the CM effect is incomplete. While the range of the cross-section variation r must still reflect the extent to which the initial-state wave function is distorted, when this distortion is severe the origins of σ modification may be more complicated than just the disturbing of matrix element cancellation at the CM.

It is possible that the Ag $4d$ wave function is surprisingly extended and thus has reduced absolute σ values, with respect to the atomic case, as well as a quenched CM effect. It is also possible that the $\sigma_{4d}(h\nu)$ curve reported by Abbati *et al.*¹³ may suggest similar properties for the $4d$ states in Mo metal. Certainly the shape of σ_{4d} for Mo metal is similar to an sp -type monotonic decrease with increasing photon energy, but the absolute magnitude of σ_{4d} is not available for comparison with other systems.

V. CONCLUSION

Photoemission in the Cooper-minimum region has been used to study the Ag $4d$ -derived virtual bound states in the random substitutional $\text{Cd}_{97}\text{Ag}_3$ and $\text{Al}_{95}\text{Ag}_5$. The $4d$ states of Ag when dilute in the free-electron metal Al are found to exhibit a deep atomlike Cooper minimum indicative of a highly atomic $4d$ wave function. When alloyed to the d -electron metal Cd the $4d$ states of Ag ex-

hibit a weak Cooper minimum, showing that the presence of the host (Cd) $4d$ band severely distorts the Ag $4d$ wave functions. We have observed further that for the $\text{Cd}_{97}\text{Ag}_3$ alloy the cross sections for the Ag $4d$ states are consistently smaller than for the same orbital on the Cd sites. We conclude that the environmental effects on $\sigma(h\nu)$ are evident throughout the photon-energy range, and are not restricted to the CM region. More work on other metals and alloys is required before a systematic understanding of the effect reported here is achieved.

We also conclude that it is desirable to have an internal reference in each spectrum, to avoid the use of large correction factors, and we point out the importance of measuring relative cross sections in the study of alloys. At present, little attention has been devoted to a theoretical explanation of solid-state effects on photoionization cross sections. The CM effect provides a sensitive probe

of wave-function information, which would otherwise be difficult to obtain experimentally or theoretically. We hope that the increasing number of experimental studies in this area will help stimulate more theoretical involvement and help to develop a potentially very fruitful technique.

ACKNOWLEDGMENTS

This work was supported in part by a Twinning Contract between the Physics Department of Liverpool University, Trinity College Dublin, the Politecnico di Milano, and the University of Rome (la Sapienza) funded by the Science programme of the European Commission. The SERC is acknowledged for providing access to the beamline, at the SRS and for partial financial support for two of us (R.J.C. and J.A.E.).

- ¹J. W. Cooper, *Phys. Rev.* **128**, 681 (1962).
- ²U. Fano and J. W. Cooper, *Rev. Mod. Phys.* **40**, 441 (1968).
- ³H. Wright, P. Weightman, P. T. Andrews, W. Folkerts, C. F. J. Flipse, G. A. Sawatzky, D. Norman, and H. Padmore, *Phys. Rev. B* **35**, 519 (1987).
- ⁴W. Folkerts, D. van der Marel, C. Haas, G. A. Sawatzky, D. Norman, H. Padmore, H. Wright, and P. Weightman, *J. Phys. F* **17**, 657 (1987).
- ⁵G. K. Wertheim, *Phys. Rev. B* **36**, 4432 (1987).
- ⁶D. Greig, B. L. Gallagher, M. A. Howson, D. S.-L. Law, D. Norman, and F. M. Quinn, *Mater. Sci. Eng.* **99**, 265 (1988).
- ⁷L. Duò, J. A. Evans, A. D. Laine, G. Mondio, P. T. Andrews, D. Norman, and P. Weightman, *J. Phys. Condens. Matter* **3**, 989 (1991).
- ⁸G. Rossi, I. Abbati, L. Braicovich, I. Lindau, and W. E. Spicer, *Solid State Commun.* **39**, 195 (1981).
- ⁹J. N. Miller, S. A. Schwarz, I. Lindau, W. E. Spicer, B. De Michelis, I. Abbati, and L. Braicovich, *J. Vac. Sci. Technol.* **17**, 920 (1980).
- ¹⁰G. Rossi, I. Lindau, L. Braicovich, and I. Abbati, *Phys. Rev. B* **28**, 3031 (1983).
- ¹¹P. S. Wehner, J. Stöhr, G. Apai, F. R. McFeely, R. S. Williams, and D. A. Shirley, *Phys. Rev. B* **14**, 2411 (1976).
- ¹²R. F. Davis, S. D. Kevan, B.-C. Lu, J. G. Tobin, and D. A. Shirley, *Chem. Phys. Lett.* **71**, 448 (1980).
- ¹³I. Abbati, L. Braicovich, G. Rossi, I. Lindau, U. del Pennino, and S. Nannarone, *Phys. Rev. Lett.* **50**, 1799 (1983).
- ¹⁴T. A. Carlson, A. Fahlman, M. O. Krause, T. A. Whitley, and F. A. Grimm, *J. Chem. Phys.* **81**, 5389 (1984).
- ¹⁵I. Abbati, L. Braicovich, C. Carbone, J. Nogami, J. J. Yeh, I. Lindau, and U. del Pennino, *Phys. Rev. B* **32**, 5459 (1985).
- ¹⁶M. O. Krause, W. A. Svensson, T. A. Carlson, G. Leroi, D. E. Ederer, D. M. P. Holland, and A. C. Parr, *J. Phys. B* **18**, 4069 (1985).
- ¹⁷M. Ardehali and I. Lindau, *J. Electron Spectrosc. Relat. Phenom.* **46**, 215 (1988).
- ¹⁸G. N. Kwawer, T. J. Miller, M. G. Mason, Y. Tan, F. C. Brown, and Y. Ma, *Phys. Rev. B* **39**, 1471 (1989).
- ¹⁹M. Ardehali and I. Lindau, *Phys. Rev. B* **42**, 1097 (1990).
- ²⁰J. Friedel, *Nuovo Cimento Suppl.* **7**, 287 (1958).
- ²¹P. W. Anderson, *Phys. Rev.* **124**, 41 (1961).
- ²²P. Weightman and P. T. Andrews, *J. Phys. C* **13**, 3529 (1980).
- ²³P. H. Hannah and P. Weightman, *J. Phys. F* **16**, 1015 (1986).
- ²⁴M. R. Howells, D. Norman, G. P. Williams, and J. B. West, *J. Phys. E* **11**, 199 (1978).
- ²⁵U. del Pennino, S. Nannarone, L. Braicovich, I. Abbati, G. Rossi, and I. Lindau, *J. Electron Spectrosc. Relat. Phenom.* **37**, 389 (1986).
- ²⁶R. P. Gupta and A. J. Freeman, *Phys. Rev. Lett.* **36**, 1194 (1976).
- ²⁷J. J. Yeh and I. Lindau, *At. Data Nucl. Data Tables* **32**, 1 (1985).
- ²⁸P. A. Wolff, *Phys. Rev.* **124**, 1030 (1961).
- ²⁹A. M. Clogston, B. T. Matthias, M. Peter, H. J. Williams, E. Corenzwit, and R. C. Sherwood, *Phys. Rev.* **125**, 541 (1962).
- ³⁰M. Vos, D. van der Marel, and G. A. Sawatzky, *Phys. Rev. B* **29**, 3073 (1984).
- ³¹R. A. Pollak, S. Kowalczyk, L. Ley, and D. A. Shirley, *Phys. Rev. Lett.* **29**, 274 (1972).